

# EVOLUTION OF THE SNS SUPERCONDUCTING PROTON LINAC\*

Yanglai Cho<sup>†</sup> for the SNS Collaboration  
Argonne National Laboratory, Argonne, IL USA  
and

Oak Ridge National Laboratory, Oak Ridge, TN USA

## Abstract

The construction of the Spallation Neutron Source (SNS) at Oak Ridge, Tennessee, USA, is a USDOE multilaboratory project carried out by ANL, BNL, LANL, LBNL, ORNL, and TJNAF. The construction is to be completed in the year 2006. The baseline SNS linac is capable of delivering an H<sup>+</sup> ion beam of 1 GeV in energy and 1.4 MW in beam power with a 60 Hz repetition rate. The linac consists of warm and cold parts. The cryogenic linac section accepts beam of ~180 MeV from the warm linac and accelerates it to 1 GeV. Furthermore, the performance of the linac can be upgraded to 1.3 GeV in energy and ~4 MW in beam power with an appropriate upgrade of the rf system. The evolution of the linac design and status of the construction are presented. A detailed description of prototype cavity development is found elsewhere in these proceedings [1].

## 1 INTRODUCTION

The Spallation Neutron Source (SNS) is an accelerator-based pulsed neutron source, which provides thermal neutrons to condensed matter research. The baseline accelerator system is to deliver a beam power greater than 1.4 MW and consists of an H<sup>+</sup> ion source, a radio-frequency quadrupole (RFQ), a 1 GeV linac, a compressor ring and associated beam transport systems. The time-averaged beam current is 1.4 mA. The SNS facility parameters are shown in Table 1.

In January 2000, the main section of the SNS linac was changed from normal conducting copper technology to a superconducting technology after extensive reviews. The new linac baseline configuration consists of a drift tube linac (DTL), which accelerates an incoming 2.5 MeV beam from a RFQ to 70 MeV, a coupled cavity linac (CCL), which accelerates the 70 MeV beam to 186 MeV, and a superconducting (SC) section, which accelerates the 186 MeV beam to 1 GeV.

The superconducting portion consists of two parts, a medium- $\beta$  and a high- $\beta$  section. In spite of the fact that there have been many design studies for high-power proton superconducting linacs during the past decade, the SNS linac will be the first high-intensity proton superconducting linac.

Table 1: The SNS Facility Parameters

Proton beam energy on target	1.0	GeV
Proton beam current on target	1.4	mA
Power on target	1.4	MW
Pulse repetition rate	60	Hz
Beam macropulse duty factor	6.0	%
Average current in macropulse	26	mA
H <sup>+</sup> peak current in Front End	>38	mA
Chopper beam-on duty factor	68	%
RFQ output energy	2.5	MeV
Front End + linac length	335	m
DTL output energy	87	MeV
CCL output energy	186	MeV
SC linac output energy	1.0	GeV
HEBT length	170	m
Accumulator ring circumference	248	m
Ring fill time	1	msec
Ring beam extraction gap	250	nsec
RTBT length	150	m
Number of protons/pulse	$1.5 \cdot 10^{14}$	
Proton pulse width on target	695	nsec
Target material	Hg	

In the early summer of 1999, a working group was formed to assess the possibility of changing the SNS linac configuration from a warm linac [2] to a cryogenic linac.

The working group met in August 1999 at Argonne and in September 1999 in Newport News. The participants of the working group came from ANL, Cornell University, JLab, and LANL from the US and, DESY, INFN-Milan and JAERI from abroad.

At the initial meeting, the working group had agreed on the starting parameters and configuration of the linac for the optimizations and made work assignments to refine the performances and authorship of the design document. The design report [3] was completed in November 1999, and it was approved by a peer-review committee in December 1999. The formal baseline change took place in January 2000, and the SRF linac project commenced on February 1, 2000.

Step-by-step discussions, which led to the present linac configuration, are presented in the report together with the status of the construction.

\* Work supported by the U.S. DOE Office Basic Energy Sciences under contract DE-AC05-00OR22725.

<sup>†</sup> [yc@aps.anl.gov](mailto:yc@aps.anl.gov) or [yhc@ornl.gov](mailto:yhc@ornl.gov)

## 2 LIMITATION OF SRF STRUCTURE

The theoretical limitation of the performance of the SRF structure comes from the rf magnetic field at the inner surface of the cavity. According to theory this field must be below the superheating field of the superconductor (200 – 240 mT for Nb.) This allowable peak surface magnetic field translates into the allowable peak surface electric field  $E_{\text{peak}}$ , which is ~ 100 to 120 MV/m.

Then the achievable accelerating electric field  $E_{\text{acc}}$  can be determined from the geometry of cavity and  $E_{\text{peak}}$ . A typical geometrical factor varies from 2 to 3.

The cavities under development at the TESLA Test Facility (TTF) in DESY, Hamburg, Germany, have achieved  $E_{\text{acc}} > 25$  MV/m for their recent production batches. Since TTF cavities have a geometrical factor equal to 2, the peak surface fields,  $E_{\text{peak}}$ , of these cavities were all greater than 50 MV/m [4].

## 3 TRANSIENT TIME FACTOR

The velocity of particles being accelerated in an electron linac is almost constant and is close to the velocity of light. This constant velocity simplifies electron linac design considerations. On the other hand, the varying particle velocity in proton linacs introduces two additional concepts that must be incorporated in the design consideration.

The first concept is the cavity- $\beta$ , which is a geometrical property of the cavity designed for a particular velocity of particle ( $\beta$ ). For example, a given  $\beta$  dictates the cavity inter-iris separations.

The second concept is introduction of the transient time factor,  $T$ . The energy gain of a particle that has gone through one rf cycle can be expressed:

$$\Delta V = T V \cos(\phi)$$

Where  $V$  is the accelerating voltage, and  $\phi$  is the beam phase with respect to the rf wave. The transient time factor,  $T = \beta/4$  when the particle velocity equals the geometrical velocity of the cavity,  $\beta_g$ , and  $T < \beta/4$  for all other  $\beta$ .

This transient time factor consideration demonstrates the fact that the acceleration is most efficient when  $\beta = \beta_g$  and is not efficient for all other  $\beta$ s. This is the reason why a warm proton linac has many segments with each segment having a difference  $\beta_g$  so that the rf power is made more efficient.

## 4 CHOICE OF PARAMETERS

### 4.1 Choice of rf Frequency

Historically, the frequency of the linac rf system was based on the availability of high-power rf sources. In the late 1950s and early 1960s, a 201.25 MHz source was one of the most powerful rf sources available to accelerator communities, and, during this period, a number of linacs

were built with the 201.25 MHz system. This includes the ANL 50 MeV, BNL 50 MeV, LANSCE 200 MeV DTL, FNAL 200 MeV and BNL 200 MeV linacs. The LANSCE 800 MeV linac uses 805 MHz, which is the fourth harmonic of the 201.25 MHz.

On the other hand, during the advent of electron storage rings, 350 MHz klystrons have become widely available for high-power operations. Consequently, many of the planned high-power proton linacs have been designed around 350 and 700 MHz rf source combinations.

During the conversion to the cryogenic linac, the possibility arose of switching the linac rf system from 402.5/805 MHz to the more commonly available 350/700 MHz rf sources. The decision was not to switch the frequency because the linac front-end system was already under construction with the 402.5 MHz system. Switching to a new frequency would add an additional year to the construction period.

### 4.2 Choice of Constant Energy Gain vs. Constant Gradient

At first glance, constant energy gain/m appears much simpler and attractive. However due to the transient time factor,  $T$ , when each cavity is forced to have the same energy gain, the cavity with a smaller  $T$  must have higher  $E_{\text{acc}}$  and higher  $E_{\text{peak}}$  in order to make the constant energy gain. Instead, a decision was made to design a constant gradient system for the linac. In this way, the variation of  $E_{\text{peak}}$  among cavity to cavity is minor and stays within a reasonable range.

### 4.3 Number of Cavity Velocity Groups

Previous studies have shown that a linac with three velocity group sections can accelerate a proton beam to 1 GeV [5]. A section with  $\beta_g$  of ~ 0.5 (low  $\beta$ ) for beam energy 70 to 180 MeV, a section with  $\beta_g \sim 0.6$  (medium  $\beta$ ) for 180 to 350 MeV, and  $\beta_g \sim 0.8$  (high  $\beta$ ) for beam energy greater than 380 MeV.

### 4.4 Number of Cells per Cavity and Number of Cavities per Cryomodule

The design rule was to minimize the number of ends of the cavities and also minimize the number of ends of the cryomodule while taking into account ease of construction. This rule is to minimize the head load of the accelerating structure due to the ends.

Minimizing the number of ends of cavities means that each cavity should have the largest possible number of cells. On the other hand, ease of construction implies that the number of cells per cavity should be less. After some discussion, 6-cell cavities were chosen for handling ease during the construction.

To minimize the number of cavities per cryomodule and yet keep the length of a cryomodule short enough to handle during construction and maintenance, the decision was made to have three cavities in the low- $\beta$  module and

four cavities in the high- $\beta$  module. The lengths of modules are sufficient to use a doublet quadrupole transverse focusing system to transport the beam through the linac. A choice was made to have a warm quadrupole system rather than a cold one to avoid a potential complexity of the cold cavity-cold magnet. The transverse focusing system in the warm section is the FODO system, and a smooth transition is designed into the system.

#### 4.5 Choice of Accelerating Gradient

Before studying beam dynamics, rf power source, etc., the design gradient has to be decided as a starting point for a refined study.

There have been two sets of data on cavity gradients, both from L-band electron accelerating structures of CEBAF and the TTF. Although the Nb surface magnetic field is the determining factor for cavity performance, surface peak electric field is used in the consideration for conveniences. The value of  $E_{\text{peak}}$  can be directly converted to  $E_{\text{acc}}$  by a simple division with the cavity geometrical factor, which varies between 2 to 4.

Past experience with the CEBAF cavities shows that  $E_{\text{acc}}$  of  $\sim 7\text{-}8 \text{ MV/m} \pm 10\%$ , which translates to  $E_{\text{peak}}$  of 14 to 16 MV/m  $\pm 10\%$ , can be achieved. However the most recent experience at TTF was that  $E_{\text{acc}}$  of  $> 20 \text{ MV/m}$  or  $E_{\text{acc}} > 40 \text{ MV/m}$  was achieved in their third production batch.

After lengthy discussions, the working group agreed to use  $E_{\text{peak}} \sim 27.5 \text{ MV/m} \pm 10\%$ . Then  $E_{\text{acc}}$  will be determined by the geometrical factor from the cavity shape.

Recently, the SNS has decided to use  $E_{\text{peak}} \sim 35 \text{ MV/m} \pm 10\%$ . This can be achieved in two different ways. Since the DESY people have demonstrated that a good buffered chemical polishing (BCP) can provide cavities with  $E_{\text{peak}} > 50 \text{ MV/m}$ , the SNS team should be able to achieve the same level of performance. The second way is to electropolish the cavities. Currently, SNS team is implementing an electropolishing process.

An electropolishing process developed and perfected by KEK gives 15 to 20% better cavity performance based on a limited number of samples. Several laboratories including CERN, JLab (SNS), KEK, DESY are implementing this process to achieve a higher gradient.

#### 4.6 Choice of Input Energy and Cavity Beta Groups

As noted in Section 3.3, several previous studies of high-intensity superconducting proton linacs have led to the conclusion that three velocity groups (low- $\beta$ , medium- $\beta$ , and high- $\beta$ ) of cavities would be sufficient to accelerate protons to above the 1 GeV energy range with an input beam from a warm linac of  $\sim 70 \text{ MeV}$ . Since acceleration efficiency of a DTL is excellent for energy up to 70 or 100 MeV protons, it is customary to use a DTL of this energy range as the first section of cold linac designs.

Typically, a low- $\beta$  section covers proton energy ranges of 70 to 100 MeV, a medium- $\beta$  section for 180 to 350

MeV, and high- $\beta$  section for 350 MeV or higher. These are starting points of iterative optimizations involving consideration of the number of cryomodules in each section, as well as input and output energies.

For the SNS, a decision was made not to pursue a low- $\beta$  section because, unlike medium or high- $\beta$  cavities, it requires extensive R&D, and the SNS construction schedule lacked sufficient time to carry out R&D on low- $\beta$  cavities. The reason for requiring additional R&D is that lower  $\beta$  cavities are difficult to build due to the physical dimensions of the cavities and lack of mechanical strength. This lack of mechanical strength causes the Lorentz detuning. So instead of the low- $\beta$  section, the design is to use the already developed CCL.

Table 2 shows input and output energies of each linac section.

Table 2: Input/output energies of each linac section

Section	$\beta$	$\beta$ range	Input (MeV)	Output (MeV)
DTL			2.5	86
CCL			87	186
Med.- $\beta$	0.61	0.55-0.70	186	394
High- $\beta$	0.81	0.70-0.87	394	1000

#### 4.7 rf Issues

There are two key rf issues that need to be addressed. The first is consideration of the rf power requirement and power sources. Since all rf power goes to the beam being accelerated, the power requirement for each cavity is the power gain of the beam being accelerated.

The choice on hand is whether to have an rf system in which a higher power klystron supplies energies to several cavities by dividing the power (one klystron for several cavities) or a system in which each cavity is energized by a single klystron (one-on-one).

In this consideration, one must take into account the fact that one  $\beta$  group of cavities accelerates a wide range of the particle velocities. The consequence of having a wide velocity range for a single geometrical  $\beta$  is a need for controlling both the rf voltage and rf phase of individual cavities independently.

Controlling the rf phase and amplitude of an individual cavity is straightforward for the one-on-one system.

However for a one klystron multicavity system, such control is nontrivial and requires at least two phase shifters for each cavity to adjust the phase and amplitude of the rf independently. The complexity of the waveguide system offsets any potential cost saving of the one klystron-many cavities arrangement. So the decision is to use the one-on-one arrangement.

The second rf issue was the choice of high-power couplers and geometrical configuration. The decision was to copy the best performing coupler available from anywhere. The KEK B-Factory coupler operating at 508 MHz cw was the best available in September 1999, and the decision was to copy it and scale it to 805 MHz operation.

An additional change implemented is to feed the rf power from below rather than from above as was done at KEK. This is done to eliminate or minimize possible dust contamination of the cavity.

#### 4.8 Other Items Requiring Attention

Since the stored energy in a cavity is proportional to the square of the Efield, and the mechanical force on the cavity wall is also proportional to  $E^2$ , a frequency shift due to the Lorentz force,  $\Delta f$ , is proportional to  $E_{acc}^2$  or  $\Delta f = kE_{acc}^2$ . Thus the energy gain/cell is less than the desired value due to the frequency shift. The remedy is to prevent the deformation of the cavity by mechanical means (e.g., stiffeners or feed-back and feed-forward) and/or to have additional rf power to make up the  $\Delta E$  loss due to Lorentz detuning.

Microphonics is amplification of ambient noise by the cold cavity. This microphonics also shifts the cavity resonance frequency. The remedy is to reduce noise sources, shift eigen frequencies of the cavity by mechanical design, and have enough rf power to compensate the insufficient energy gain per cavity. This rf gymnastics involves both feedback and feed forward.

### 5 ADVANTAGES OF SRF LINAC FOR SNS

There are several advantages for switching to the cold linac from the warm linac. Here are some examples of the advantages.

Early industrial participation without too much training of industry - A MW class warm proton linac was last constructed in the mid-1960s. This means that industrial capability for the construction of a warm linac without intensive training by laboratory is nonexistent. On the other hand, superconducting rf technology was developed by JLab in the 1980s and most recently by DESY in conjunction with industry.

Construction and operating costs are less – The expected power consumption saving is about 10 to 12 MW. This translates to about \$3M/year of the power cost savings. The construction cost savings comes from a shorter linac enclosure and klystron building and reduction of utility needs.

The availability of a SRF linac is designed to be higher than the warm linac – The use of one klystron per cavity enables operation with one or two klystron(s) turned off by re-phasing the neighboring cavities. This capability is due to the fact that the superconducting linac has a very large velocity acceptance and reserve capability. The reserve capacity comes from the fact that all rf power coming to the cavity goes to the beam, and when higher beam energy or higher beam current is needed, just adding more rf power would be sufficient.

Energy upgrade – At a later date, the linac can be energy-upgraded by increasing the rf power. The SNS accumulator ring can be operated at a 4 MW level when the linac delivers a 1.3 GeV beam.

Energy stability – The SNS accumulator ring imposes stringent requirements on the linac beam energy and its

spread jitters in order to avoid the incoming beam missing the stripper foil. The stripper foil converts the incoming H<sup>-</sup> ion beam to a proton beam at a designated location of the ring trajectory. The studies have shown that for individual control of phase and amplitude of the accelerating rf, the SRF linac provides a better beam performance.

Ultrahigh vacuum of the cryogenic system – For an accelerator of this power level, one of the most important design considerations is potential uncontrolled beam loss within the accelerator itself. Past experience has shown that a tolerable beam loss for hands-on maintenance is about 1 W/m or less. The ultrahigh vacuum from the cryogenic system creates negligible beam-gas interaction.

Control of beam loss – The cold linac has a larger bore (diameter of 10 cm) compared to that of the warm linac (diameter of 3.5 cm). A consequence of this larger bore is that all particles, including possible halo particles, are accelerated and transported through the linac. If the halo particles do exist, these can be collected at a designated location in the high-energy beam transport line.

### 6 STATUS OF R&D AND CONSTRUCTION

The schedule for the SNS SRF linac consists of a two-year prototyping R&D period and a two-year period of cavity construction along with design/construction of the cryogenic system and transfer lines.

Some of the key prototyping items include four medium- $\beta$  and two high- $\beta$  cavities. A complete 3-cavity medium- $\beta$  cryomodule is formed using three out of four cavities. For prototyping of the high- $\beta$  cryomodule, due to lack of time, prototyping was not planned. In addition, 10 high-power input couplers are to be prototyped and tested. A detailed description of the prototyping is in these proceedings.

Figure 1 shows the SNS prototype cavities: (a)  $\beta = 0.61$  and (b)  $\beta = 0.81$ . As for electromagnetic performance based on the vertical tests without titanium He vessels, both the medium- and high- $\beta$  cavities exceeded the design goals after proper treatments.

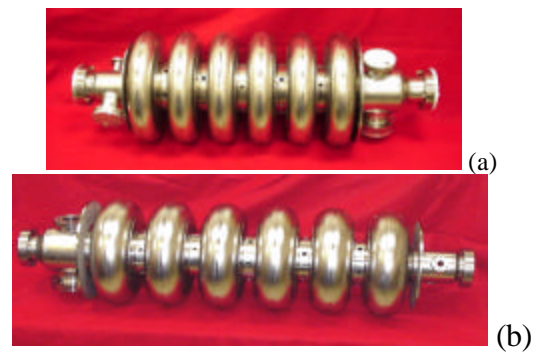


Figure 1: SNS prototype cavities: (a)  $\beta=0.61$  and (b)  $\beta=0.81$ .

Figures 2 and 3 show  $Q_0$  vs.  $E_{acc}$  curves for the  $\beta = 0.61$  cavity and the  $\beta = 0.81$  cavity, respectively. The design goals for both types of cavities are clearly marked in the figures.

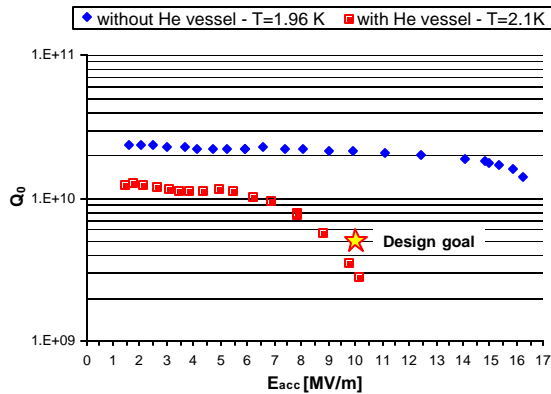


Figure 2: SNS  $\beta=0.61$  vertical test results.

As shown in Figure 2, a medium- $\beta$  cavity performance is degraded after welding of the He vessel. The cause of this may be dust involved during welding of the vessel and is under study.

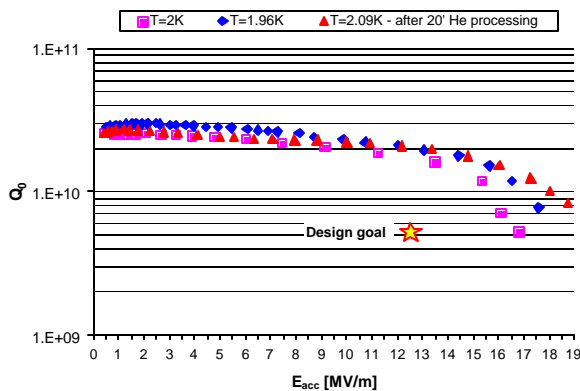


Figure 3: SNS  $\beta=0.81$  vertical test results.

The test result to date on the high- $\beta$  cavity shows that the  $Q_0$  and  $E_{acc}$  perform substantially above the design goals, as indicated in Figure 3.

For all important power couplers, prototyping work is progressing well, and a prototype coupler is shown in Figure 4. As noted earlier, this is a scaled and modified version of the KEK B-Factory coupler.

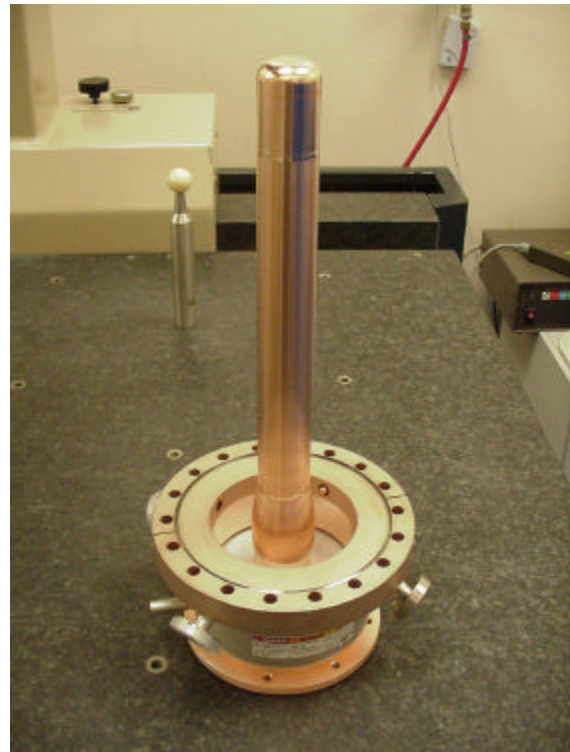


Figure 4: Prototype SNS power coupler.

## 7 SUMMARY

The evolution of the SNS superconducting linac design and the summary description of prototyping are presented. The schedule calls for the start of cryomodule installation in September 2003, and the linac cool down in March 2004. The entire SRF system should be operational in September 2004, and the linac beam should be available to transport to the ring in December 2004.

The SNS work is the result of hard work put forth by all partner laboratories and their staff.

## 8 REFERENCES

- [1] G. Ciovati, et al., in these Proceedings
- [2] SNS CDR, <http://www.sns.gov>
- [3] Y. Cho et al., Superconducting Radio Frequency Linac for the SNS, SNS-SRF-99-101 (1999)
- [4] TESLA Technical Design Report, DESY Report, 2001
- [5] For example, T. P. Wangler, SRF-99 Workshop